Four-Wave Mixing and its Applications

C. W. Thiel

The process of four-wave mixing is discussed. The theoretical basis of FWM is developed followed by an examination of common experimental methods based upon FWM processes. Some of the applications and uses of FWM are presented.

Key Words: Four-Wave Mixing, Coherent Raman Processes

Introduction

The field of nonlinear optics[1, 2, 3] was ushered in with the development of the first laser by Maimen[4] in 1960. Although nonlinear optical effects had been known as early as the nineteenth century (The Pockels and Kerr effects), only DC fields could be produced with enough intensity to reach the regime of nonlinear optical response. Due to this deficiency, nonlinear optics remained unexplored until the classic experiment by Franken and co-workers[5] in which second-harmonic generation was demonstrated in quartz with the use of a ruby laser. With a readily available source of coherent optical radiation that exhibited nearly monochromatic characteristics, reports of new phenomena quickly became common in the professional literature. Among the first of these were observations of two-photon absorption by Kaiser and Garrett,[6] stimulated Raman scattering by Ng and Woodbury,[7] third-harmonic generation by Maker and co-workers,[8] and anti-Stokes frequency mixing by Terhune and co-workers.[9] Soon after the first observations of optical nonlinearities were made, a theoretical explanation was provided based upon the nonlinear response of electron oscillators in the atomic Coulomb field. The field of nonlinear optics has continued to grow at a tremendous rate since its inception in 1961 and has proven to be a nearly inexhaustible source of new phenomena and optical techniques.

The particular areas of nonlinear optics which will be explored in this paper are the phenomena arising from the interaction of four coherent optical fields through the third order nonlinear susceptibility. An indication of the importance that the scientific community places on this topic was given in 1981 when Nicholaas Bloembergen and Arthur Schawlow received the Nobel Prize in physics for their work in this field.[10] This field includes many diverse processes such as degenerate four-wave mixing, stimulated Raman scattering, and Raman induced Kerr effects. These processes have proven to be of utility in a great number of applications including optical processing, phase conjugate optics, real-time holography, and the measurement of atomic energy structures and decay rates. This paper will examine the basic theory of coherent third order nonlinear

processes, the most common of the nonlinear techniques employed, and some of the applications of these techniques.

Theory

The concept of three electromagnetic fields interacting to produce a fourth field is central to the description of all four-wave mixing processes. Physically, we may understand this process by considering the individual interactions of the fields within a dielectric medium. The first input field causes an oscillating polarization in the dielectric which re-radiates with some phase shift determined by the damping of the individual dipoles; this is just traditional Rayleigh scattering described by linear optics. The application of a second field will also drive the polarization of the dielectric, and the interference of the two waves will cause harmonics in the polarization at the sum and difference frequencies. Now, application of a third field will also drive the polarization, and this will beat with both the other input fields as well as the sum and difference frequencies. This beating with the sum and difference frequencies is what gives rise to the fourth field in four-wave mixing. Since each of the beat frequencies produced can also act as new source fields, a bewildering number of interactions and fields may be produced from this basic process. A mathematical model of a system's ability to support the various mixing processes is needed in order to explain the observed four-wave mixing phenomena.

The traditional method of modeling an optical material's nonlinear response is to expand the induced polarization as a power series in the electric field strength.[11, 12, 13]

$$\vec{P} = \chi^{(1)} \cdot \vec{E} + \chi^{(2)} \cdot \vec{E}\vec{E} + \chi^{(3)} \cdot \vec{E}\vec{E}\vec{E} + ... \qquad (1)$$

The expansion coefficients are known as susceptibilities in analogy to classical linear electromagnetic theory. This method assumes that the higher order susceptibilities grow progressively smaller so that the power series exansion converges to a finite polarization. This will be the case when the Rabi frequency is small compared to the homogeneous linewidths of any material resonances near the fields' frequencies.[12] This is true for most of the cases of interest, although important processes such as self-induced transparency occur when this condition is violated. In general, the susceptibilities are tensor objects that relate the different fields' directions and frequencies to the direction and strength of the induced polarization. The lowest order nonlinear susceptibility $\chi^{(2)}$ is a third rank tensor that has 27 elements. Many of these elements are determined by the symmetry of the optical medium which it describes,[11] and all the elements vanish in materials with inversion symmetry (such as gases and liquids).

The third order nonlinear susceptibility $\chi^{(3)}$ is responsible for four-wave mixing processes.[14] In general, $\chi^{(3)}$ is a fourth rank tensor with 81 elements,[15] and each of these elements consists of a sum of 48 terms. This staggering number of terms is drastically reduced through material symmetries and resonance, but unlike $\chi^{(2)}$, $\chi^{(3)}$ may have nonzero elements for any symmetry. Explicit expressions for the terms have been

published,[16] and each term has a typical form with three resonant factors in the denominator.

$$\chi^{(3)} = \frac{NL}{6\hbar^3} \sum_{g,k,n,j} \frac{\mu_{gk}\mu_{kn}\mu_{nj}\mu_{jg}\rho^0_{gg}}{[\omega_{kg} - \omega_1 - i\Gamma_{kg}][\omega_{ng} - i\Gamma_{ng} - (\omega_1 - \omega_2)][\omega_{jg} - i\Gamma_{jg} - (\omega_1 - \omega_2 + \omega_3)]}$$

$$+ 47 \text{ other terms} \qquad (2)$$

The summation in (2) is taken over all states of the oscillator, and N is the oscillator density, μ_{gk} is the electric dipole matrix element between states g and k, ω_{kg} is the frequency of the transition from g to k, Γ_{kg} is the damping of the off-diagonal element of the density matrix that connects g to k, and $\omega_{1,2,3}$ are the frequencies of the fields. The tensor properties of the susceptibility are derived from the vector properties of the dipole matrix elements in (2). The primary difference between the 48 terms is the ordering of the frequencies involved in the summation. A method of using diagrammatic representations for these terms in calculating perturbations to the density matrix has been suggested by Yee et. al.[17] (similar to Feynman diagrams in particle physics). The susceptibility is usually simplified further by only considering terms which have small factors in the denominators due to resonance with oscillator frequencies.[18] For example, Raman processes are described by the terms which contain ω_1-ω_2 and ω_3-ω_2, while two-photon absorption is described by terms that contain ω_1+ω_3.

In order to understand the four-wave mixing process, a closer examination of the third order nonlinear polarization must be made. The general form of the polarization may be written as shown in (3).

$$P_i(\omega_4, \vec{r}) = \tfrac{1}{2}\, \chi^{(3)}_{ijkl}(-\omega_4, \omega_1, -\omega_2, \omega_3) E_j(\omega_1) E^*_k(\omega_2) E_l(\omega_3) \exp[i(\vec{k}_1 - \vec{k}_2 + \vec{k}_3)\cdot\vec{r} - i\omega_4 t]$$
$$+ \text{c.c.} \qquad (3)$$

This nonlinearity describes a coupling between four waves, each with its own direction of propagation , polarization, and frequency. This expression for the polarization immediately gives insight into the nature of measured four-wave mixing signals. Since the physical quantity that is measured by experiment is the field intensity, the observed signal will be proportional to $|\chi^{(3)}|^2$, the product of the three field intensities, and a "phase matching" factor. This functional dependence is often used as a quick method of verifying that an observed signal is actually due to a third order mixing effect.

Now, if this nonlinear polarization is substituted into Maxwell's equations, a set of four coupled wave equations may be found for the fields. The form of the equations is simplified by defining nonlinear scalar coupling coefficients and a wave vector mismatch,[14]

$$\chi^{NL}_{1234} \equiv \hat{e}_1\hat{e}^*_2 : \chi^{(3)}(-\omega_4, \omega_1, -\omega_2, \omega_3) : \hat{e}_3\hat{e}^*_4$$

$$\chi_{ij}^{NL} \equiv \hat{e}_i \hat{e}_i^* : \chi^{(3)}(-\omega_i, \omega_i, -\omega_j, \omega_j) : \hat{e}_j \hat{e}_j^* \tag{4}$$

$$\Delta kz \equiv (\vec{k}_1 - \vec{k}_2 + \vec{k}_3 - \vec{k}_4) \cdot \vec{r}$$

where e_i is the polarization vector of the i^{th} field. The equations for the field magnitudes may now be written in the following form (using the slowly varying envelope approximation).

$$\begin{aligned}
\frac{\partial E_1}{\partial z} + \frac{1}{v_1}\frac{\partial E_1}{\partial t} &= 2\pi i \frac{\omega_1}{n_1 c}[\chi_{1234}^{NL} E_2 E_3^* E_4 \exp(-i\Delta kz) + \sum_{j=1}^{4} \chi_{1j}^{NL} E_1 E_j E_j^*] \\
\frac{\partial E_2}{\partial z} + \frac{1}{v_2}\frac{\partial E_2}{\partial t} &= 2\pi i \frac{\omega_2}{n_2 c}[\chi_{1234}^{NL} E_1 E_3 E_4^* \exp(+i\Delta kz) + \sum_{j=1}^{4} \chi_{2j}^{NL} E_2 E_j E_j^*] \\
\frac{\partial E_3}{\partial z} + \frac{1}{v_3}\frac{\partial E_3}{\partial t} &= 2\pi i \frac{\omega_3}{n_3 c}[\chi_{1234}^{NL} E_1^* E_2 E_4 \exp(-i\Delta kz) + \sum_{j=1}^{4} \chi_{3j}^{NL} E_3 E_j E_j^*] \\
\frac{\partial E_4}{\partial z} + \frac{1}{v_4}\frac{\partial E_4}{\partial t} &= 2\pi i \frac{\omega_4}{n_4 c}[\chi_{1234}^{NL} E_1 E_2^* E_3 \exp(+i\Delta kz) + \sum_{j=1}^{4} \chi_{4j}^{NL} E_4 E_j E_j^*]
\end{aligned} \tag{5}$$

In most of the common four-wave mixing processes, these equations are simplified since some of the frequencies, wave vectors, and polarizations are degenerate.

The equations in (5) cannot be solved in general, so the usual approach taken is to assume plane wave solutions and that the energy transferred from the input fields to the fourth field is a negligible fraction of the total energy of the fields. With these assumptions, we may decouple the equations (5) and solve for the four fields. This gives the equations (6) for the field intensities,[19]

$$\begin{aligned}
I_{1j} &= I_{1j}(0)\exp(-\alpha_1 L) \\
I_{2k} &= I_{2k}(0)\exp(-\alpha_2 L) \\
I_{3l} &= I_{3l}(0)\exp(-\alpha_3 L) \\
I_{4i} &= \frac{L^2}{4}\exp(-\alpha_4 L)\left|\chi_{ijkl}^{(3)}(\omega_4) E_{1j}(0) E_{2k}(0) E_{3l}^*(0)\right|^2 \times G(\Delta kL)
\end{aligned} \tag{6}$$

$$G(\Delta kL) = \frac{1 + \exp(-\Delta\alpha L) - 2\exp(-\frac{1}{2}\Delta\alpha L)\cos(\Delta kL)}{\frac{1}{4}L^2(\Delta k^2 + \frac{1}{4}\Delta\alpha^2)} \tag{7}$$

where α_i is the absorption coefficient at ω_i, L is the effective length of overlap of the four fields, and G(ΔkL) is the phase matching factor. The reduction of equations for the input fields to the Beer-Lambert law is a direct consequence of the assumption of negligible energy transfer to the output field. Notice that the phase matching factor (7) reduces to the familiar form $\text{sinc}^2(\frac{1}{2}\Delta kL)$ when there is no absorption of the fields.

The assumption of plane wave solutions limits the validity of (6) since the fields used experimentally are invariably Gaussian.[20] In order to apply this theory to Gaussian beams, the interaction length must be much smaller than the Rayleigh range so that phase fronts may be approximated as planar. Modifications of the theory due to focusing effects have been calculated by Bjorklund[21] for the case of isotropic media..

Efficient coupling between the four waves described by (6) may only occur when energy and momentum are both conserved:[12] $\omega_4 = \omega_1 - \omega_2 + \omega_3$, and $\vec{k}_4 = \vec{k}_1 - \vec{k}_2 + \vec{k}_3$. Another equivalent way of understanding these conditions is by realizing that since the energy transfer is a coherent process, all four waves must maintain a constant phase relative to the others in order to avoid any destructive interference. These constraints are embodied in the phase matching factor of equation (7). G(ΔkL) only has an appreciable magnitude near ΔkL=0; thus, the output field is completely decoupled from the input fields for large phase mismatches. ΔkL=0 may be achieved by either having a very short overlap length, or choosing a small wave vector mismatch. Phase matching[22] is the process of choosing the directions, and polarizations in birefringent media, in order to eliminate the wave vector mismatch. Figure 1 is a pictorial representation of the wave vector mismatch: situation (a) shows a finite wave vector mismatch, while (b) demonstrates the corresponding phase matched case. The constraints imposed by phase matching are responsible for the highly directional nature of the signals produced by four-wave mixing and the ease of spatially separating the output fields. Phase matching may also be used as a spectral filter since only a very narrow frequency band may be phase matched along a particular direction.[13]

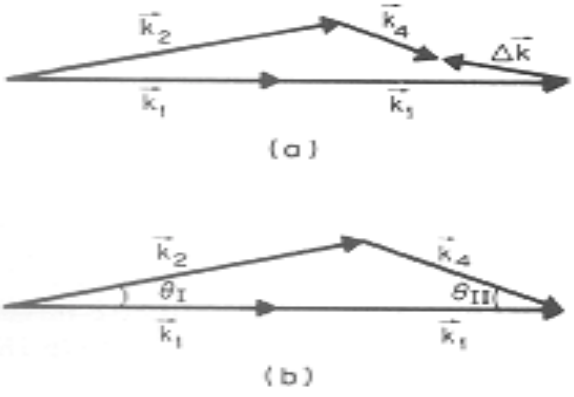

Figure 1. (from reference [13]) This is a typical CARS phase matching diagram where (a) displays a wave vector mismatch of Δk, and (b) is the perfectly phase matched case.

Four-Wave Mixing Processes

Now that the basic theory of four-wave mixing has been presented, examination should be made of the most common four-wave mixing processes used in experimental science. These processes are summarized in table 1 and figure 10.

CARS-"Coherent Anti-Stokes Raman Spectroscopy"

Coherent anti-Stokes Raman spectroscopy is the most common of all the four-wave mixing processes. The CARS process involves the input of two fields of frequencies ω_1 and ω_2 ($\omega_1>\omega_2$). Two photons of frequency ω_1 interact with a single photon of frequency ω_2 to create an output field with a frequency of $\omega_s=2\omega_1 - \omega_2$. In this process, the two input frequencies are chosen so that $\omega_1 - \omega_2$ is near a transition of the dielectric medium—this is a coherent version of Raman scattering. This process is represented by situation (b) in figure 2. Since there are only two input beams, phase matching is achieved through selection of the relative angle and polarization of the two beams as in (b) of figure 3. The primary advantage of CARS is the large signal produced.[15] Due to the efficient transfer of energy to the signal field and the directional nature of the coherent beams, CARS may be as much as a billion times more sensitive than spontaneous Raman scattering (COORS). The main disadvantage of CARS is the inevitable contributions to the signal from the non-resonant terms in equation (2). These effects can cause a variable background signal that obscures the resonant signal. The non-resonant terms may also "interfere" with the resonant terms causing the observed lineshapes to be distorted from their true shapes. A diagram of a typical CARS experimental setup is given in figure 4.

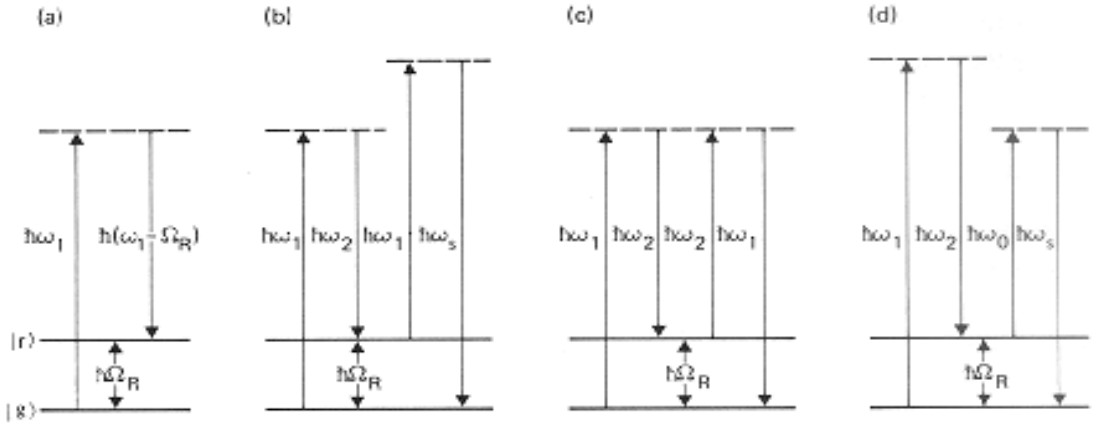

Figure 2. (from reference [15]) Pictorial representation of photon interactions. (a) The spontaneous scattering mechanism giving rise to conventional old-fashioned ordinary Raman spectroscopy (COORS). (b) The process in coherent anti-Stokes Raman spectroscopy (CARS); this would represent coherent Stokes Raman spectroscopy (CSRS) if $\omega_1<\omega_2$. (c) The process in stimulated Raman gain spectroscopy (SRS), the inverse Raman effect (TIRE), and Raman-induced Kerr effect (RIKE). (d) General four-wave mixing.

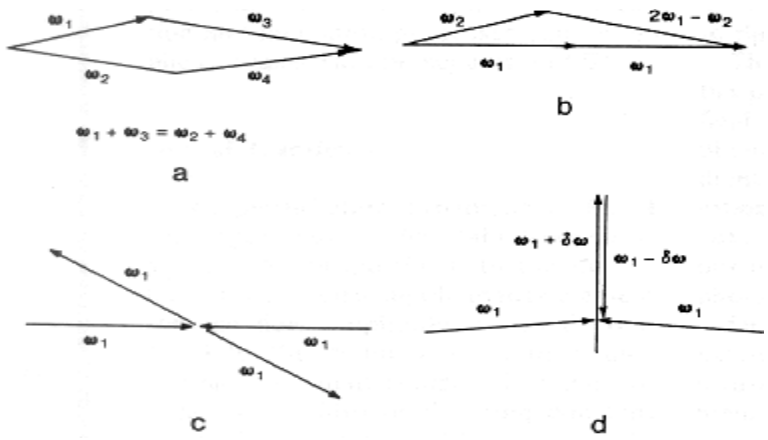

Figure 3. (from reference [3]) Typical phase matching geometries for various four-wave mixing processes. (a) General four-wave mixing (often referred to as BOXCARS). (b) CARS or CSRS (referred to as folded BOXCARS or ARCS). (c) Degenerate four-wave mixing (DFWM). (d) Two-photon absorption (TPA).

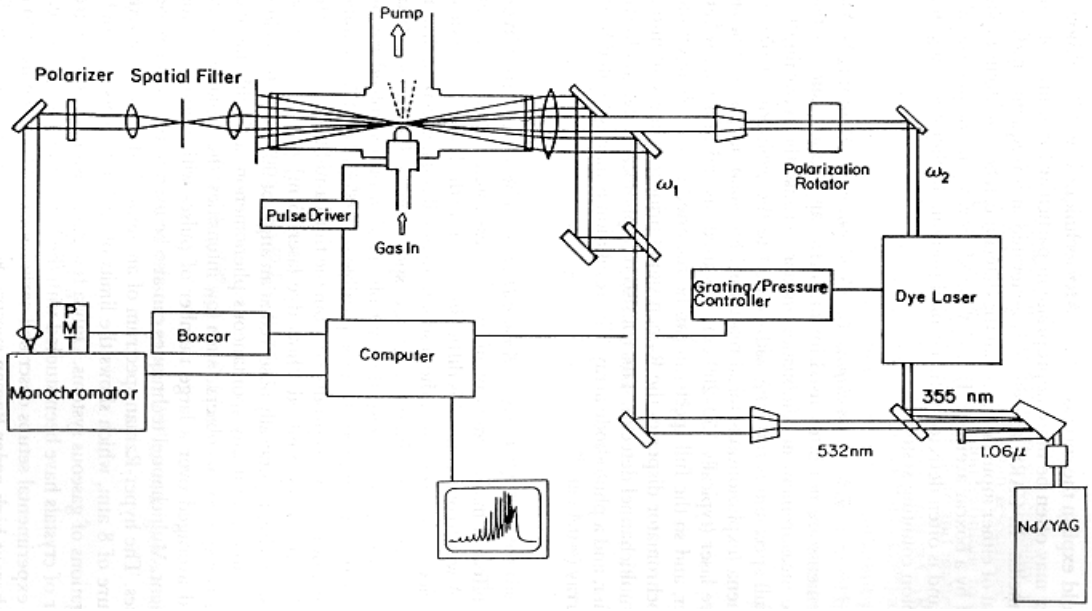

Figure 4. (from reference [23]) Typical CARS apparatus at Oregon State University

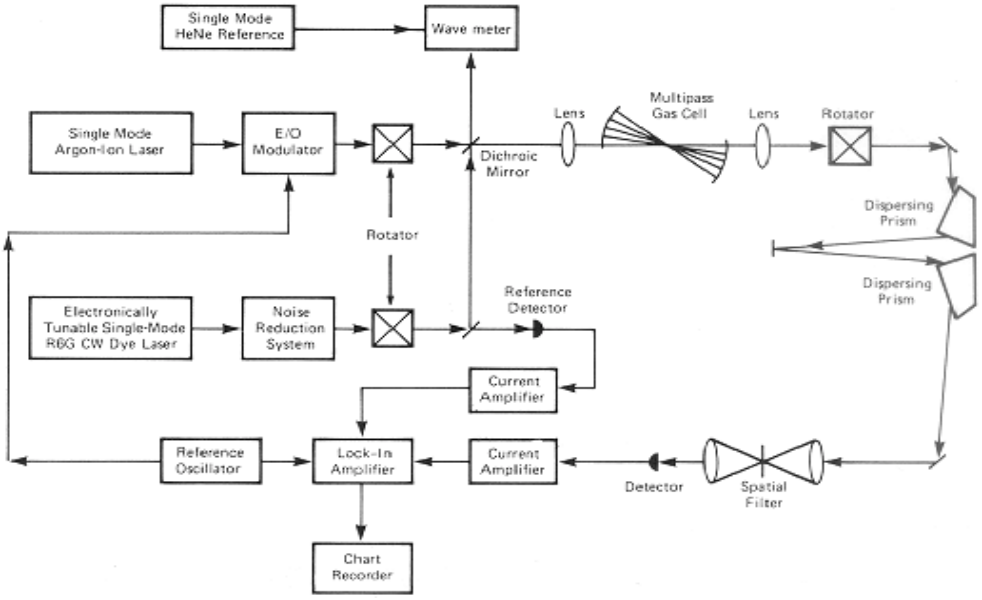

Figure 5. (from reference [24]) Experimental apparatus for performing high-resolution SRS with cw lasers

CSRS-"Coherent Stokes Raman Spectroscopy"

Coherent Stokes Raman Spectroscopy (CSRS—pronounced "scissors") is the same as CARS except with $\omega_1<\omega_2$: the output is at the Stokes frequency.

SRS-"Stimulated Raman Gain Spectroscopy"

Modern techniques of SRS employ stable cw probe lasers to detect the small changes (1 part in a million) in intensity due to a Raman gain induced by a second pump laser.[25] This process is represented by (c) of figure 2. This technique relies on the resonant enhancement of the coupling of the pump field to the probe field as the difference in frequencies between the two fields approaches a transition of the material. This coupling causes a gain in the probe beam which may then be detected with a photodiode. The advantages of this process are that it is insensitive to the non-resonant background signal present in CARS, the observed signal is linearly proportional to the Raman scattering cross section, and it is also insensitive to depolarization of the fields. An additional advantage of SRS is the automatic fulfillment of phase matching due to the double degeneracy of the mixing frequencies. The main disadvantages of SRS is that it requires an extremely stable cw probe laser in order to obtain high-resolution spectra, and the observed signal gain may be complicated due to fluorescence or "hot luminescence." An example of a SRS Raman spectrometer is shown in figure 5.

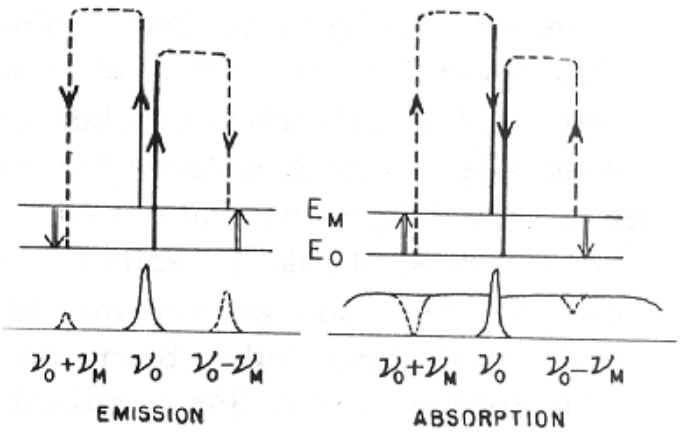

Figure 6. (from reference [26]) Depiction of Raman absorption and emission spectra obtained by TIRES. The central peak represents the laser source and the smooth lamp spectrum is shown superimposed on the absorption diagram. The two observed peaks correspond detection of a single Raman resonance by both Stokes and anti-Stokes emission or absorption.

TIRES-"The Inverse Raman Effect Spectroscopy"

The inverse Raman effect is an alternate method of detecting the presence of pump induced Raman gain that was first used by Jones and Stoicheff in 1964.[26] The most common method of TIRES uses a laser and an intense broadband source as a probe. The laser plays the same role that the probe beam plays in SRS, while the broadband source acts as the pump. The frequencies of the broadband source that differ from the laser frequency by a material resonance will couple to the laser producing Raman gain. This coupling of energy into the laser field will cause an apparent loss at the resonant frequencies in the broadband source's spectrum. This process is depicted in figure 6. The main advantages of this method over SRS are that it may be used to obtain an entire Raman spectrum at once, and it avoids many of the problems due to the background Raman fluorescence present in other techniques.

RIKES-"Raman Induced Kerr Effect Spectroscopy"

The use of an intense electric field to induce birefringence in a medium has been known since the middle of the nineteenth century: the optical Kerr effect. Four-wave mixing also has the potential to induce a birefringence in a material, and this is the basis for RIKES.[27] When a four-wave mixing process is resonant with a Raman transition, such as in SRS, the strong interaction induces a birefringence in the medium, and thus causes the polarizations of the input fields to be altered. This process may be predicted from the tensor properties of the third-order susceptibility; in general, the induced polarization will have a component perpendicular to the polarization of the input field. This can be detected with great sensitivity by measuring the transmission through crossed polarizers. The main disadvantage of RIKES is that it is sensitive to stress induced birefringence in the medium. A typical RIKES apparatus is diagrammed in figure 7.

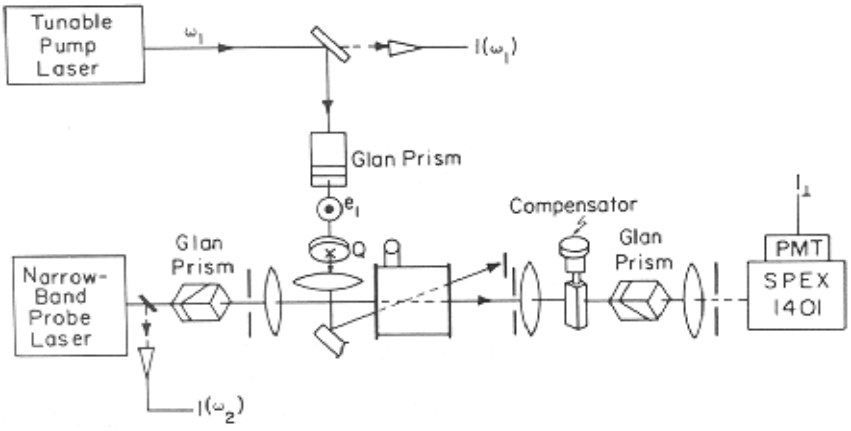

Figure 7. (from reference [27]) Typical RIKES experimental setup.

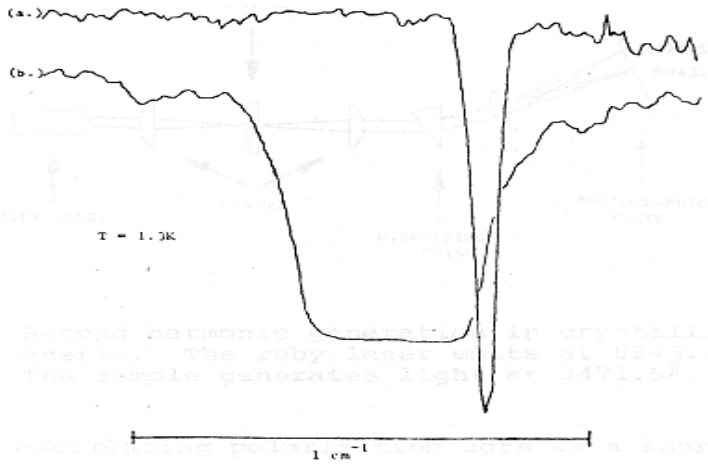

Figure 8. (from reference [19]) An examination of the $^5D_4$ Γ_1 state of $LiTbF_4$ using FWM. (a) Four-wave mixing signal, and (b) single-photon absorption signal. The observed narrowing of the FWM signal is due to the frequency selectivity of the phase matching condition.

FWM-"Four-Wave Mixing"

The term "four-wave mixing" is usually reserved for the interaction of four spatially or spectrally distinct fields. FWM reduces to the previously discussed processes when two or more of the frequencies are degenerate. FWM may be used to probe either one-photon resonances or two-photon resonances in a material by measuring the resonant enhancement as one or more of the frequencies are tuned. By tuning the frequencies to multiple resonances in the material, excited state cross sections, lifetimes, and linewidths may be measured.[18, 19] Another unique advantage of FWM is that Raman cross sections

may be directly compared by tuning the two difference frequencies to the two Raman transitions of interest (ω_1-ω_2 and ω_3-ω_2). FWM also has the advantage of eliminating the non-resonant background signals present in the other methods. The main disadvantage of FWM is the complications involved in simultaneously overlapping three coherent beams while maintaining the phase matching condition (BOXCARS). Experimental data obtained through FWM are shown in figure 8 and figure 9.

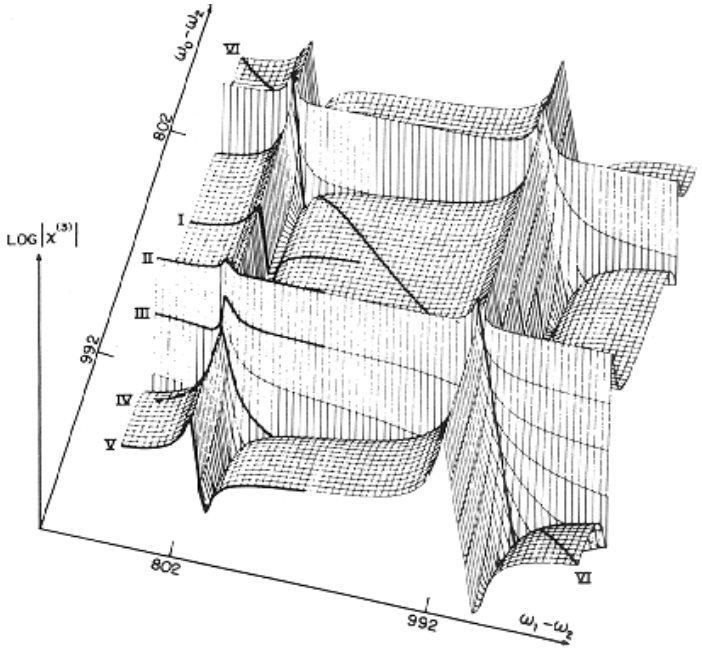

Figure 9. (from reference [28]) Two-dimensional plot of the dispersion of $|\chi^{(3)}_{1111}|^2$ versus the two difference frequencies in a 1:1 mixture of benzene and cyclohexane. The heavy lines show data obtained by FWM and path VI corresponds to CARS. The ratio of the Raman cross sections of benzene and cyclohexane was determined from such plots to be 3.45:1.

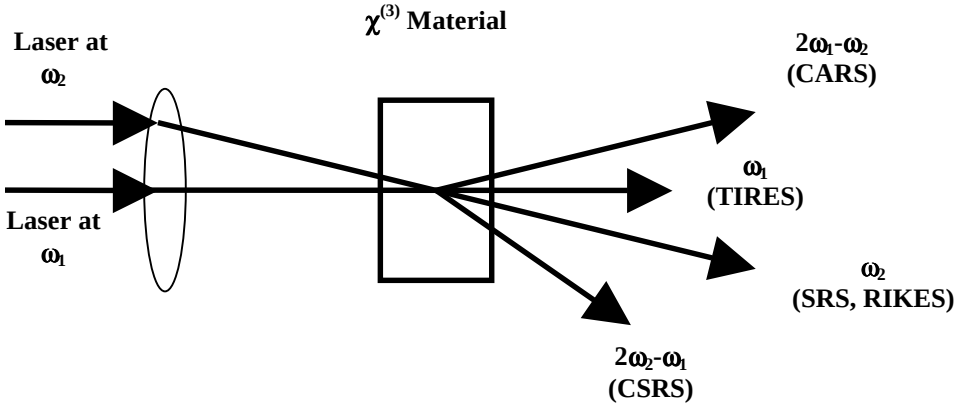

Figure 10. Diagram of coherent Raman processes and the relative orientation of output signals detected in the different methods of Raman spectroscopy ($\omega_1 > \omega_2$ and ω_1- ω_2 is near a Raman resonance).

Table 1. Spectroscopic Applications of Four-Wave Mixing

Nonlinear Interaction	Quantity Varied	Quantity Measured	Information Obtained
Sum frequency mixing $\omega_4 = 2\omega_1 + \omega_2$	ω_2	Intensity at ω_4	Energy level structure near ω_4
Third-harmonic generation $\omega_4 = 3\omega_1$	ω_1	Intensity at ω_4	Energy levels near $2\omega_1$ with same parity as ground state
Difference frequency mixing (CARS) $\omega_4 = 2\omega_1 - \omega_2$	ω_2	Intensity at ω_4	Raman energy levels, susceptibilities, lifetimes, etc.
Four-wave mixing (FWM) $\omega_4 = \omega_1 + \omega_2 - \omega_3$	$\omega_1 - \omega_3$ $\omega_2 - \omega_3$	Intensity at ω_4	Raman levels, susceptibilities, lifetimes, etc.
Raman-induced Kerr effect (RIKE) $\omega_2 = \omega_1 + \omega_2 - \omega_1$	ω_2	Polarization changes at ω_2	Raman levels, susceptibilities, lifetimes, etc.
Raman gain spectroscopy (SRS) $\omega_2 = \omega_1 + \omega_2 - \omega_1$	ω_2	Gain at ω_2	Raman levels
The inverse Raman effect spectroscopy (TIRES) $\omega_2 = \omega_1 + \omega_2 - \omega_1$	ω_1	Loss at ω_1	Raman levels

Applications

In this section, some of the many applications of the four-wave mixing processes will be discussed.

Phase-Conjugation

Phase-conjugation is the name given to the process of reversing the phase development of an electromagnetic wave.[11, 29] This is equivalent to reversing the relative signs of the spatial and temporal development of the wave. A phase-conjugated wave would appear to travel "backward" in time. The usefulness of this process arises when a wave is distorted by traveling through an inhomogeneous medium. If the distorted wave

could be phase-conjugated, the progress of the phases introduced by the medium would be reversed, and thus the wave would develop back to its original undistorted state.

Four-wave mixing is one method of producing a phase-conjugate of an incoming wave. If we consider equations (5) and (6), and the situation shown in (a) of figure 11, we realize that the field E_4 will be the phase conjugate of E_3 if E_1 and E_2 are plane waves (they contain no spatial information) and if all of the waves are the same frequency (degenerate FWM). Thus, by using two counterpropagating pump beams and satisfying the phase matching condition, the nonlinear medium may be used as a phase-conjugate reflector. This method may also be used to remove individual distortions by replacing the pump waves with phase distorted plane waves.[30] The use of the distorted reference waves allows the phase distortion to be selectively erased.

One application of the FWM phase-conjugate reflector is as an intra-cavity element of a laser system. By using a phase-conjugate mirror as the rear-reflector in a laser cavity, any distortions introduced during the lasing process may be removed as they re-traverse the cavity. The success of this process is shown in figure 12.

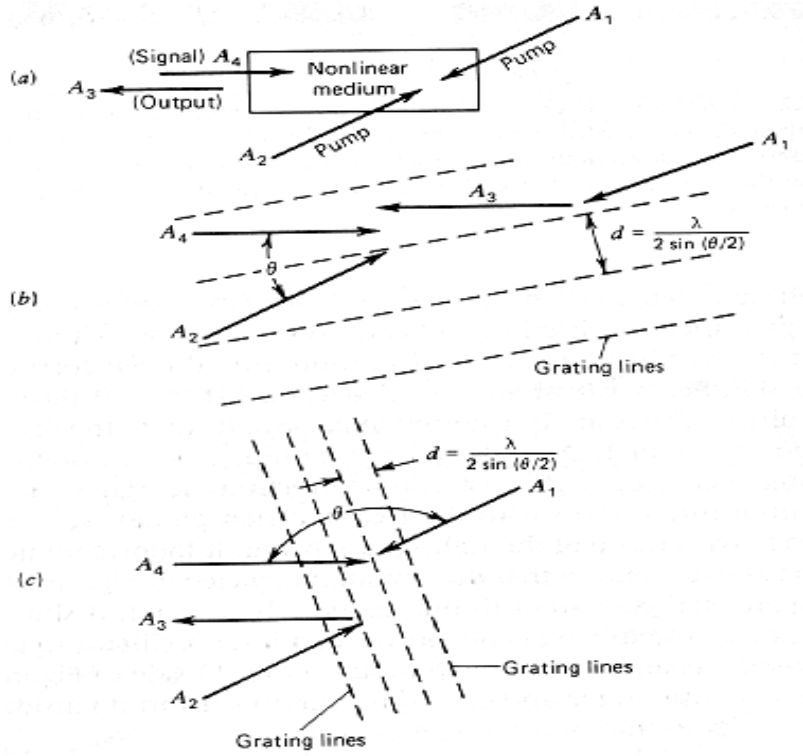

Figure 11. (from reference [11]) (a) The conventional geometry of phase conjugation through FWM. (b) Beams 2 and 4 interfere to form an index grating $A_2A_4^*$. Beam 1 is Bragg-diffracted from the grating to yield the output phase-conjugate of A_4 (which is A_3). (c) Beams 1 and 4 interfere to form an index grating $A_1A_4^*$. Beam 2 is Bragg-diffracted from the grating to yield the output phase-conjugate of A_4 (which is A_3).

The FWM phase-conjugate reflector may be simplified even further through the use of a photorefractive crystal. In this scheme of phase conjugation, the input wave is scattered in the crystal and then internally reflected by crystal faces cut at the phase matching angle. These reflected waves then acts as the pump waves for FWM; the crystal acts as a self-pumped phase-conjugate reflector.[31, 32] The use of a photorefractive material greatly enhances the self-pumping since its refractive index is more easily modulated by the interfering fields, thus enhancing the diffraction into the pump field. An excellent example of the performance of a self-pumped phase conjugate mirror is shown in figure 13.

Real-time Holographic Imaging

Degenerate FWM may also be used for real-time holographic imaging.[34, 35] The analogy between FWM and holography may be understood from figure 11. In either (b) or (c), it is shown that the interference of two of the waves act to form a real-time grating in the optical medium. This "index grating" may be viewed as an intensity dependent modulation of the susceptibility (and thus the index of refraction) due to the nonlinear interaction between the fields and the dielectric medium. The third wave is then Bragg-diffracted from this grating to produce the fourth wave. Thus, just as in traditional holography, both the spatial and phase information of an input beam reflected from an object is stored in the interference pattern. This information may then be used to reconstruct the original wave by diffracting the third wave from the interference pattern.

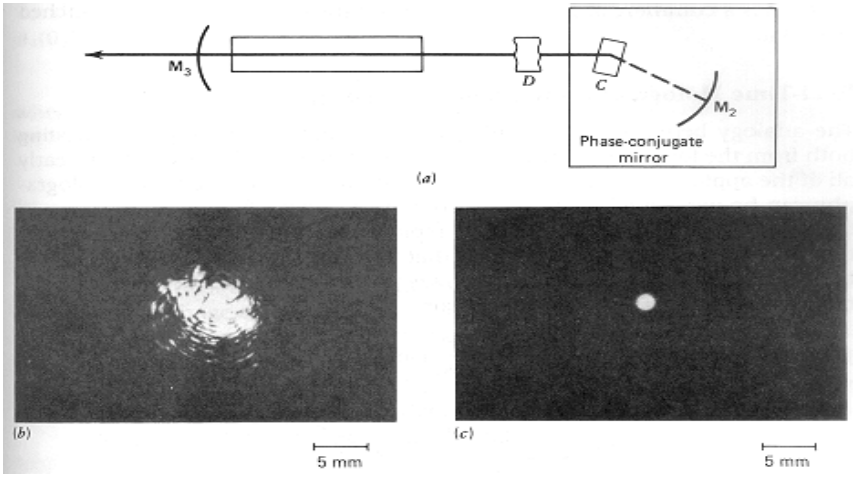

Figure 12. (from reference [33]) (a) An argon laser gain tube with a distortion D, a phase-conjugating crystal C, and a feedback mirror M_2. (b) The highly degraded output beam from M_3 when a conventional mirror is used as the rear-reflector. (c) The beam regains its diffraction-limited shape in the presence of the distortion when the phase-conjugate reflector is used.

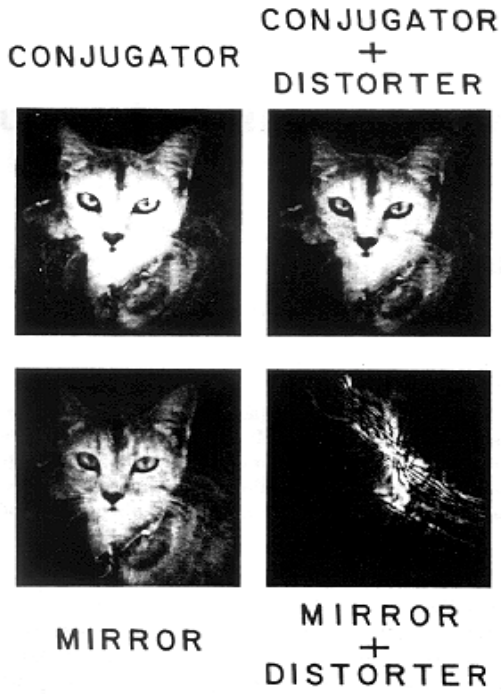

Figure 13. (from reference [31]) An example of the distortion removing capabilities of the self-pumped phase-conjugate mirror.

Real-time Image Processing

Another technique which utilizes the analogy between holography and FWM is real-time image processing.[36] The concepts of Fourier optics predict that if an image is passed through a lens, the Fourier transform of the image will be formed in the focal plane of the lens. If a nonlinear medium is placed in the focal plane of a lens, and three waves containing spatial information are focused through the lens, an induced polarization given by equation (3) will radiate a fourth wave which will be proportional to the product of the Fourier transforms of the original waves. Now, if this fourth wave is passed back through the lens, the spatial variation of the resulting wave (in the focal plane) will be the inverse Fourier transform of the product of the Fourier transforms of the input waves. Therefore, from basic Fourier analysis we know that the output wave will be the convolution of two of the waves correlated with the third (this is because one wave enters as a complex conjugate in the polarization). By choosing one of the waves to have a simple Fourier transform, either spatial correlations or convolutions may be performed instantly. Figure 14 is an example of correlations and convolutions performed using this method.[37]

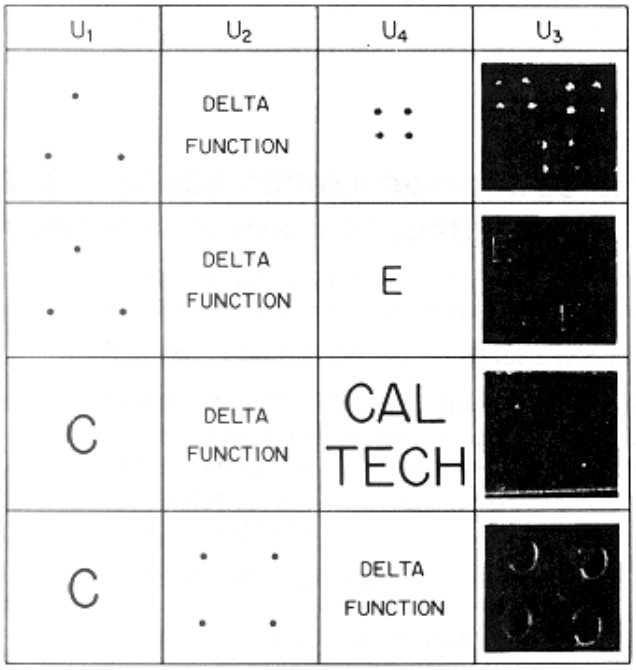

Figure 14. (from reference [37]) An example processing using FWM. The first three columns are the input waves. The last column is the convolution of the first two correlated with the third.

Generation of Coherent Sources in the VUV and IR

FWM and the related Raman processes may be used as methods for producing coherent light sources in the extreme regions of the spectrum. Four-wave mixing with a resonant Raman transition is commonly used to transfer energy from a tunable dye laser into the Stokes wave, thus producing a tunable source of coherent IR radiation. Third-harmonic generation is also a special case of degenerate FWM which is used to produce a tunable source of coherent radiation in the VUV region of the spectrum.[38]

Measurement of Excited State Lifetimes and Dephasing Rates

A very useful spectroscopic application of four-wave mixing is the measurement of lifetimes and dephasing rates. One method for doing this involves temporally separating the three input beams and measuring the resulting output (time-resolved CARS). A FWM output may only occur if the atomic states interacting with the applied fields maintain their coherence, thus the dephasing rate may be determined. A second method of determining homogeneous dephasing rates relies on the spectral selectivity of the phase matching condition. If the interaction length of the FWM process is increased, Δk must become smaller in order to effectively couple the input fields to the output field; thus, by choosing a large enough L, the spectral width of the FWM signal should reduce to the homogeneous linewidth limit. An additional method of simultaneously determining both the natural lifetime and the dephasing rate using FWM has been

suggested by Yajima and Souma.[39] This method observes the output signal as the two difference frequencies are tuned through a material resonance. This technique has successfully been used to measure picosecond relaxation times.

Conclusion

Only a small portion of the field of four-wave mixing was sampled in this paper due to the plethora of applications that have been found for its many different manifestations. The purpose of this paper was to convey the essence of the complicated process of four-wave mixing so that the reader may gain a conceptual understanding of the many important applications that have been made of this process. This is a dynamic field that will undoubtedly continue to grow well into the future.

References

1. N. Bloembergen, editor, Proceedings of the International School of Physics Enrico Fermi Course LXIV: Nonlinear Spectroscopy, (North Holland, Amsterdam, 1977)
2. N. Bloembergen, Nonlinear Optics, (World Scientific Publishing, Singapore, 1996)
3. N. Bloembergen, "Nonlinear Optics and Spectroscopy," Science **216**, 1057-1064 (1982)
4. T. H. Maimen, "Stimulated Optical Radiation in Ruby," Nature **187**, 493-494 (1960)
5. P. A. Franken, A. E. Hill, C. W. Peters, and G. Weinreich, "Generation of Optical Harmonics," Phys. Rev. Lett. **7**, 118-119 (1961)
6. W. Kaiser and G. C. B. Garrett, "Two-Photon Excitation in CaF_2; Eu^{2+}," Phys. Rev. Lett. **7**, 229-231 (1961)
7. E. J. Woodbury and W. K. Ng, "Ruby Laser Operation in the Near IR," Proc. IRE **50**, 2367 (1962)
8. P. D. Maker, R. W. Terhune, and C. M. Savage, "Optical Third Harmonic Generation," in Quantum Electronics, edited by P. Grivet and N. Bloembergen (Columbia University, New York, 1964), pp. 1559-1578
9. P. D. Maker and R. W. Terhune, "Study of Optical Effects Due to an Induced Polarization Third Order in the Electric Field Strength," Phys. Rev. **A137**, 801-818 (1965)
10. G. B. Lubkin, "Nobel Physics Prize to Bloembergen, Schawlow and Siegbahn," Phys. Today **34** (12), 17-20 (1981)
11. A. Yariv, Quantum Electronics, (John Wiley & Sons, New York, 1989)
12. N. Bloembergen, "Conservation Laws in Nonlinear Optics," J. Opt. Soc. Am. **70**, 1429-1436 (1980)
13. J. F. Reintjes, Nonlinear Optical Parametric Processes in Liquids and Gases, (Academic Press, Orlando, 1984)

14. N. Bloembergen, “Recent Progress in Four-Wave Mixing Spectroscopy,” in Laser Spectroscopy IV, edited by H. Walther and K. W. Rothe, (Springer, Berlin, 1979), pp. 340-348
15. M. D. Levenson and S. S. Kano, Introduction to Nonlinear Laser Spectroscopy, (Academic Press, San Diego, 1988)
16. N. Bloembergen, H. Lotem, R. T. Lynch, Indian J. Pure and Appl. Phys. **16**, 151 (1978)
17. S. Y. Yee, T. K. Gustafson, S. A. J. Druet, and J-P. E. Taran, “Diagrammatic Evaluation of the Density Operator for Nonlinear Optical Calculations,” Opt. Comm. **23**, 1-7 (1977)
18. J-L. Oudar and Y. R. Shen, “Nonlinear Spectroscopy by Multiresonant Four-Wave Mixing,” Phys. Rev. A **22**, 1141-1158 (1980)
19. D. A. Ender, Doubly-Resonant Two-Photon-Absorption-Induced Four-Wave Mixing in $Tb(OH)_3$ and $LiTbF_4$, Ph. D. Thesis at Montana State University (1982) (unpublished)
20. A. E. Siegman, An Introduction to Lasers and Masers, (McGraw-Hill, New York, 1971)
21. G. C. Bjorklund, “Effects of Focusing on Third-Order Nonlinear Processes in Isotropic Media,” IEEE J. Quantum Electron. **QE-11**, 287-296 (1975)
22. J. A. Giordmaine, “Mixing of Light Beams in Crystals,” Phys. Rev. Lett. **8**, 19-20 (1962)
23. J. W. Nibler and G. A. Pubanz, Advances in Nonlinear Spectroscopy Vol. 15, ed. by R. J. H. Clark and R. E. Hester, (Wiley, London, 1988)
24. A. Owyoung, C. W. Patterson, and R. S. McDowell, Chem. Phys. Lett. **59**, 156 (1978)
25. A. Owyoung, “CW Stimulated Raman Spectroscopy,” in Chemical and Biochemical Applications of Lasers, ed. B. Moore, (Academic Press, New York, 1978)
26. W. J. Jones and B. P. Stoicheff, “Inverse Raman Spectra: Induced Absorption at Optical Frequencies,” Phys. Rev. Lett. **13**, 657-659 (1964)
27. M. D. Levenson and J. J. Song, “Coherent Raman Spectroscopy,” in Coherent Nonlinear Optics, ed. by M. S. feld and V. S. Letokhov, (Springer-Verlag, Berlin, 1980) pp. 293-373
28. H. Lotem, R. T. Lynch, and N. Bloembergen, Phys. Rev. A **14**, 1748 (1976)
29. J. AuYeung and A. Yariv, “Phase Conjugate Optics,” in Laser Spectroscopy IV, edited by H. Walther and K. W. Rothe, (Springer, Berlin, 1979), pp. 492-503
30. A. Yariv and T. L. Koch, “One-way Coherent Imaging Through a Distorting Medium Using Four-Wave Mixing,” Opt. Lett. **7**, 113-115 (1982)
31. J. Feinberg, “Self-Pumped, Continuous-Wave Phase Conjugator Using Internal Reflection,” Opt. Lett. **7**, 486-488 (1982)
32. M. Cronin-Golomb, B. Fischer, J. O. White, and A. Yariv, “Passive (Self-Pumped) Phase Conjugate Mirror: Theoretical and Experimental Investigation,” Appl. Phys. Lett. **41**, 689-691 (1982)
33. M. Cronin-Golomb, B. Fischer, J. Nilsen, J. O. White, and A. Yariv, “Laser With Dynamic Holographic Intracavity Distortion Correction Capability,” Appl. Phys. Lett. **41**, 220 (1982)
34. H. J. Gerritsen, Appl. Phys. Lett. **10**, 239 (1967)

35. A. Yariv, IEEE J. Quantum Electron. **QE-14**, 650 (1978)
36. D. M. Pepper, J. AuYeung, D. Fekete, and A. Yariv, Opt. Lett. **3**, 7 (1978)
37. J. O. White and A. Yariv, "Real-time Image Processing Via Four-Wave Mixing in a Photorefractive Medium," Appl. Phys. Lett. **37**, 5-7 (1980)
38. G. C. Bjorklund and R. R. Freeman, "cw VUV Generation and the Diagnostics of the Hydrogen Plasma," in Laser Spectroscopy IV, edited by H. Walther and K. W. Rothe, (Springer, Berlin, 1979), pp. 573-582
39. T. Yajima and H. Souma, "Study of Ultra-fast Relaxation Processes by Resonant Rayleigh-type Optical Mixing," Phys. Rev. A **17**, 309-323 (1978)